Fault Surveillance Schemes for Optical Components and Systems using Fiber Bragg Gratings and Optical Amplifiers as Monitoring Sources

F. Tong, C.K. Chan*, L.K. Chen, and D. Lam+

Department of Information Engineering
The Chinese University of Hong Kong
Shatin, Hong Kong, China

*Department of Electronic Engineering
City University of Hong Kong
Kowloon Tong, Hong Kong, China

+JDS FITEL, Inc.
Nepean, Ontario, K2G 5W8, Canada

Abstract

Several of our proposed real-time non-intrusive fault surveillance schemes for various optical components and systems are reviewed here. These schemes make use of a combination of fiber Bragg gratings as sensors and Erbium doped fiber amplifiers in the system as the light sources. By means of a hierarchical layering of fault surveillance management, these schemes can be extended to cover the entire wavelength routing network. The surveillance information can be transmitted from one managing node to another by embedding in the network signaling protocol.

Key Words: Fault surveillance; WDM components and Systems; Applications of Fiber Bragg Gratings.

1. Introduction

Wavelength division multiplexing (WDM) is a powerful technique to unleash the vast bandwidth offered by the optical fiber. At present, multi-wavelength optical-link products are available commercially, and researchers worldwide are racing towards the realization of a practical, scalable, all-optical network [1-3]. All communication systems, however capable, must demonstrate a certain degree of robustness, and issues related to surveillance, system survivability etc. must be addressed before the system can be launched. This paper reviews some of our proposed and demonstrated fault surveillance schemes for WDM components and systems. By means of hierarchical layering of fault surveillance management, the surveillance schemes can be extended to cover the entire wavelength routing network. A modified network signaling protocol to transport surveillance information will also be discussed.

There are several characteristics essential to the design of any fault surveillance scheme: (1) the sensors and its channel of delivery must be robust, (2) surveillance should be conducted in a non-intrusive manner such that data privacy can be observed, and (3) simple and low cost. Furthermore, surveillance should ideally be operated in a real-time basis, either in a continuous or periodic mode. The surveillance information can be sent to or polled by the node managers. In particular to robustness feature in (1), we should avoid the use of additional active components (e.g. monitoring light source). Any proposed surveillance scheme should also encompass all dynamic situations developed in the network, such as channel adding and dropping [4], and these features should be reflected in the design of the scheme.

Monitoring of individual components and subsystems may require optical sources. We make use of the unused portions of the amplified spontaneous emissions (ASE) of optical amplifier's (OA) as the monitoring source, as OA is an essential and commonly available component needed to compensate for the attenuation and splitting losses in the network. We also use temperature-compensated fiber Bragg grating (TC-FBG) as the optical sensor. The TC-FBGs are inserted at strategic locations in the system to provide the necessary feedback and form the monitoring channels.

Major part of this paper describes our previous fault surveillance work. Due to the diversity nature of the network components, we adopt the approach that each and every component and subsystem is monitored individually and independently, and their health status will be sent to or polled periodically by the managing nodes. Section 2 will discuss the supervisory schemes for optical cross-connects (OXC), a key component in wavelength routing network. Subsystem and system monitoring including optical fiber link and branched network will be presented in Section 3. An overall surveillance scheme for a wavelength routing network is proposed in section 4.

2. Supervision on the Component Levels

The network components discussed here include the Erbium doped fiber amplifier (EDFA), OXC, and fiber segments. EDFA and fiber segment monitoring can be grouped together, and will be discussed in section in 3.1.

Each OXC (of dimension NxN) can be formed by a total of $2N$ (N incoming and N outgoing) 1xM arrayed waveguide gratings [5] (AWG) interconnected by M banks of NxN optical space switches, assuming there are M data wavelengths (λ_1, ..., λ_M) carried on each input fiber. Identical wavelength channels but from different input fibers will be routed by the same NxN optical switch to various output fibers in accordance to the routing assignment kept in the routing control module. We assume an EDFA is to be placed at each input port so as to compensate and equalize the power among various channels [6]. We further assume that the free spectral range (FSR) of the OXC is less than the usable bandwidth of the ASE spectra of the amplifier, and the unused portion of the ASE can be used as the monitoring source. As a result, at each output port, in addition to the transmitted wavelength channels, there are multiple filtered ASE peaks, with each peak originates from different input EDFAs in accordance to the characteristics of AWG.

Two surveillance issues were investigated for OXC. The first issue deals with wavelength matching [7] and the second deals with erroneous wavelength routing [8] arising from a partial or complete failure in the optical switches in the OXC.

2.1 Wavelength Matching

Wavelength mismatch in OXC or wavelength demultiplexers is derived from fluctuations in the ambient temperature and/or device aging, causing a slight shift in the spectral responses in the AWGs. Because of the close channel spacing and non-ideal AWG's passbands, a deviation from the optimal spectral alignment in the OXC will not only lead to substantial attenuation of the transmitting signals, but also introduce severe crosstalk to the neighboring channels, greatly impairing the performance of the entire system [9].

Figure 1 illustrates the surveillance scheme and only two adjacent filtered ASE peaks at one of the OXC's output are needed. Similar scheme but with an additional light source and two dedicated output ports for monitoring was previously proposed [9]. A TC-FBG with its center wavelength matched at the midpoint (crossover wavelength) between the two adjacent filtered ASE peaks is placed at one output port (inset of Fig. 1). TC-FBG is adopted since it has a very small temperature-induced shift in center wavelength (~10^{-4}Å/^{o}C) [10]. This temperature dependence shift is about several orders of magnitude better than that of the usual SiO_2-based OXC device (~0.15 Å/^{o}C), although a high performance AWG with a temperature-dependent wavelength drift of 5.9×10^{-3} Å/^{o}C was reported recently [11]. The TC-FBG reflects the unused ASE power at that crossover wavelength back to the two corresponding input ports. The two reflected signals are then tapped off by circulators, filtered by FP filters and detected by photo-diodes as shown.

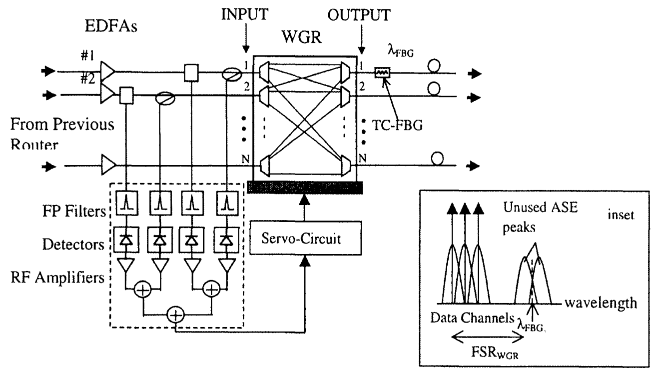

Fig.1 Proposed wavelength-matching scheme for OXC. Reproduced with permission from Ref.7. Copyright 1998, IEE.

In order to compensate for the dynamic variations in input ASE power, the two reflected signals are normalized with their respective input ASE power. The difference of the normalized signals is monitored carefully. Any change in the difference signal will trigger a servo-control circuitry, which controls the current source of a thermo-electric cooler attached to the WGR. The sign and the magnitude of the difference signal will lead to heating or cooling of the WGR until a predefined level in difference signal is reached. In this way, automatic wavelength matching is achieved without any extra reference light source. Such scheme also supports in-service monitoring and will not degrade the performance of the data channels. This monitoring method is also insensitive to the fluctuations in optical power due to channel add-drop.

Our previous investigation involves a 16 x 16 AWG with a channel spacing of 100 GHz, a 3-dB full-width of 0.4 nm, and a temperature coefficient of 0.012 nm/^{o}C to simulate the OXC. Two optical amplifiers with similar gain outputs are placed in front of input port #11 and input port #12 of the WGR. Modulated data at λ=1546.2 nm is also fed into input port #11. An FBG with a center reflection wavelength of λ_{FBG}=1559.525 nm and a 3-dB full-width of 1 nm is placed at the WGR's output port #12 where the two adjacent filtered ASE peaks considered are located at λ_1=1559.144 nm and λ_2=1559.906 nm (Fig. 1 inset) when the WGR's temperature is set at 11.5^{o}C. By activating the control-servo circuitry, the peak transmission of the WGR gradually shifts from the initial wavelength, corresponding to the initial temperature of 21.8^{o}C, to our desired wavelength assignment corresponding to 11.5°C within four minutes. Over the many hours of testing, the difference signal remains constant within ±0.01 dB, which corresponds to < ±0.001 nm in wavelength deviation (Fig. 2). Bit error rate measurements are also performed using 1-Gb/s 2^{10}-1 PRBS NRZ data with the circuitry on, and no performance degradation is observed.

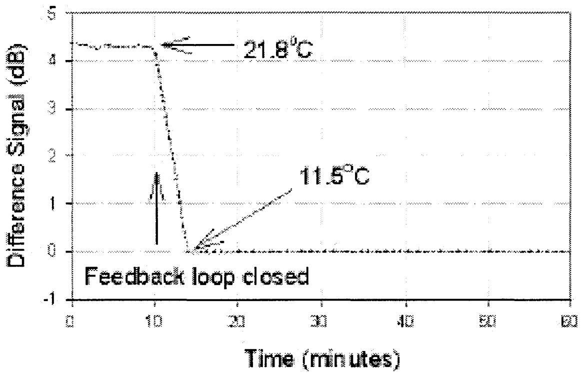

Fig. 2 Difference signal before and after feedback loop is closed. Reproduced with permission from Ref.7. Copyright 1998, IEE.

2.2 Wavelength Routing

OXC can also be at fault when the wavelength channels fail to be routed to their respective destinations in accordance to the prescribed switch settings registered in the routing control modules. These settings are used to define the optical paths for different wavelength channels from different input fibers, and will be reconfigured by the network configuration prior to each data transmission. While the transmission of the signaling control is tightly controlled, and corruption in the messages is highly unlikely, a partial or complete failure or malfunction in the optical switches in OXCs [12] will route streams of data to completely wrong destinations and lead to data loss.

Figure 3 shows the surveillance scheme for wavelength routing in OXC [8]. The basic principle of operation is to assign each input fiber of the OXC with a unique identification (ID) and will be detected and processed immediately at each output port. Thus any failure or incorrect physical connection at the switches can be detected at once by comparing the as-detected physical connection and the switch-setting information stored in the routing control module. Note that the scheme does not require tapping off any power in the data.

As shown in the figure, a unique and distinct ID will be introduced to each input fiber. To generate the ID tag for the *i*-th input port ($i=1,\ldots,N$), a small portion of the ASE is looped back to the input of $EDFA_i$ through a scanning Fabry-Perot filter (FPF) modulated at a distinct sinusoidal frequency f_i (~kHz) (see Fig. 1, inset 2). The

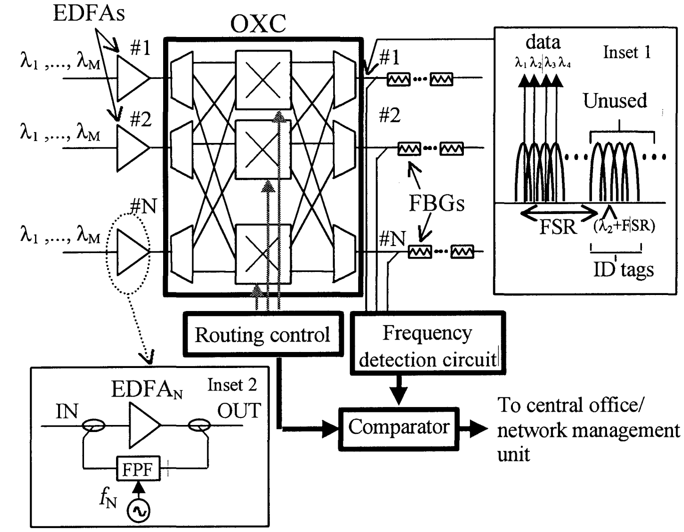

Fig. 3 Proposed optical routing path supervisory scheme for OXC. In this scheme, both routed wavelength channels and filtered ASE emerge from the output ports (inset 1). Inset 2 illustrates how a channel ID can be generated. Reproduced with permission from Ref.8. Copyright 1998, IEEE.

loopback configuration generates lasing action and the amplifier gain is clamped. The selected scanning spectral range of the FPF should cover the part of the EDFA spectrum unused by the data channels. Accordingly, for a wavelength channel at λ_k being routed by the OXC from the *i*-th input fiber to the *j*-th output fiber, there appears an ID tag on the *j*-th output fiber, located at one FSR_{AWG} from λ_k (i.e. $\lambda_{ID,k}=\lambda_k+FSR_{AWG}$; $k=1,\ldots,M$), and represented by periodic pulses at $\lambda_{ID\text{-}k}$ with a frequency of f_i. Thus, there will be *M* ID tags on each output fiber, each signifying the input fiber in which the corresponding data channel is routed from. Note that the IDs for different wavelength channels will not be mixed up because no two channels of identical wavelengths will be routed to the same output port.

On each output fiber, FBG with center wavelengths at $\lambda_{FBG}=\lambda_{ID\text{-}k}$ ($=\lambda_k+FSR_{AWG}$; $k=1,\ldots,M$) are used to drop the ID tags through circulators. The ID tags can either be demultiplexed [5], or scanned by an FPF before being detected by photodiodes. A frequency detection circuit is then used to recover the frequency of the pulses of each ID tag. By comparing this as-detected physical connection with the prescribed switch settings stored in the routing control module, any failure or error in routing can immediately be detected. Finally, a broadband rejection filter is to be placed after all the FBGs on each output fiber to eliminate the IDs, and new IDs will be generated at the input ports in the next OXC.

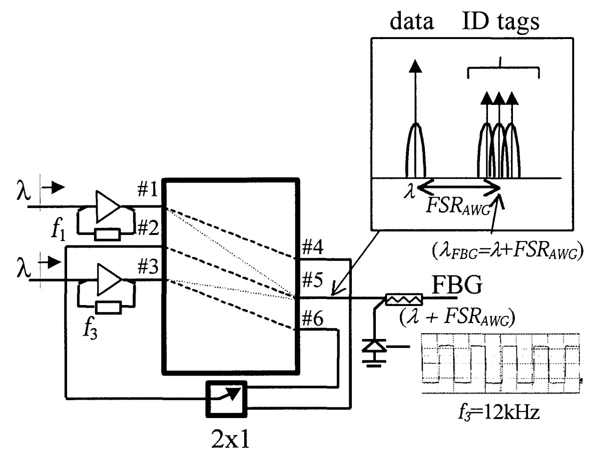

Fig. 4 Experimental setup. Reproduced with permission from Ref.8. Copyright 1998, IEEE.

Figure 4 shows our experimental configuration using the identical AWG (as described in the earlier section) in a loop-back configuration to simulate the OXC. Two EDFAs with similar gain outputs are placed at the input ports 1 and 3 of the AWG, respectively. Output ports 4 and 6, which correspond to the routing of two different data channels but of identical wavelength at λ=1546.7 nm from input ports 1 and 3, are looped back to input port 2 through a 2x1 optical switch. The resultant configuration can route the data channel λ, from either input port 1 or 3 to output port 5, depending on the state of the 2x1 optical switch. This configuration also generates three neighboring IDs at output port 5, two originating from one input EDFA and one from the other, which allows us to study the worst case scenario of neighboring ID tags. An FBG with a reflectivity of –54.68 dB, a center wavelength of $\lambda_{FBG}=\lambda_{ID}$=1559.5 nm (one FSR_{AWG} away from λ) and a 3-dB full-width of 1 nm is placed at the output port 5 for reflecting the power at λ_{ID} (ID).

To generate the channel ID, a small portion from each of the amplifiers' outputs (through a 95:5 coupler) is fed back to its input (through a 50:50 coupler). A tunable FPF of finesse 100 with a 3-dB bandwidth of 0.7 nm is placed in between the couplers at each input fiber 1 and 3. By applying a sinusoidal voltage of 0.4 V (peak-to-peak) at 10 kHz to the FPF at input port 1 and an identical voltage at 12 kHz to the FPF at input port 3, we thus obtain the IDs for the input ports 1 and 3, respectively.

A simple detection circuit is implemented after the photodiode and successfully recovers the pulse frequency of the power reflected from the FBG, which is the ID for the data channel. BER measurements were performed for the data channel at λ, externally modulated by a 1-Gb/s 2^{15}-1 PRBS NRZ data stream, for various channel ID frequencies. There are no observable power penalty arising from the FPF.

4. Subsystem and System Monitoring

Two types of WDM systems, optical fiber link and optical branched network, were considered.

3.1. Optical Fiber Links

Failure in pump laser diodes and a fiber break are the two major failure modes in an EDFA, and can be detected by means of non-intrusive real-time monitoring method using FBG and ASE of the optical amplifiers [13].

The optical transmission link (Fig. 5) under surveillance consists of N+1 EDFAs ($EDFA_0$, $EDFA_1$, ..., $EDFA_N$) and N segments of fibers. Our scheme requires an FBG inserted close to the input end of each EDFA except $EDFA_0$ which serves as the power amplifier. The distinct monitoring FBG center wavelengths, λ_1, λ_2, ..., λ_N, assigned respectively to $EDFA_1$, $EDFA_2$, ..., $EDFA_N$, are chosen from outside the EDFA's flat gain region which is reserved for data channels.

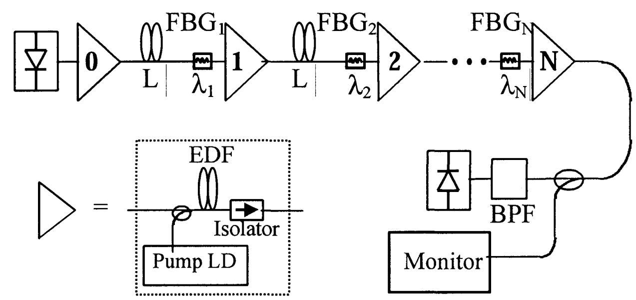

Fig. 5 Surveillance scheme for an optical transmission system.

To understand the operation principle, first we consider different ASE components at the i-th EDFA. The forward ASE from the $EDFA_{i-1}$ is filtered out by the FBG_i, resulting in a notch at λ_i of the input ASE spectrum to $EDFA_i$ [Fig. 6(a), inset (i)]. Consider a system, under normal operation, in which this notched input ASE spectrum causes $EDFA_i$ to emit less ASE at λ_i in both directions. The backward ASE from $EDFA_i$ is then reflected at λ_i by the FBG_i [Fig. 6(a), inset (ii)]. This reflection may compensate the reduced ASE spectrum at λ_i, and thus the overall output ASE spectrum of $EDFA_i$ [Fig. 6(a), inset (iii)] does not show a distinct notch at λ_i. When the forward ASE from $EDFA_{i-1}$ is too weak due to pump-laser degradation or lost by a fiber break in segment L_i, the $EDFA_i$ will emit its ASE normally without a deep notch at λ_i. The resultant spectrum from $EDFA_i$ has a strong enhanced emission at λ_i which displays as a 'spike' in the spectrum. The output spectra at the receiver end will thus be different from that of a healthy system, and these can be used for fault identification and EDFA status monitoring functions.

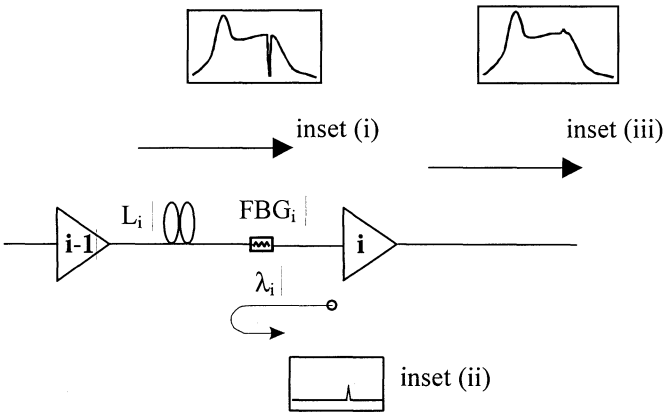

(a)

Cases	Received Spectra
(i) Healthy system	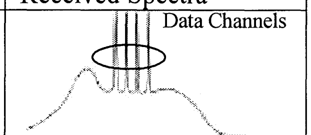
(ii) Fiber break in segment L_i	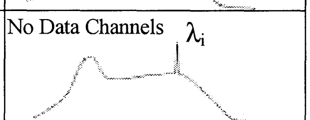
(iii) Partial failure in $EDFA_{i-1}$	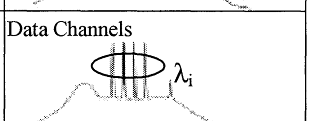
(iv) Partial failure in $EDFA_N$ (the last EDFA)	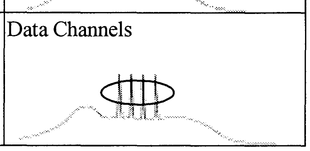

(b)

Fig. 6 (a) Operation principle of the proposed monitoring scheme. (b) Output spectra. Reproduced with permission from Ref.13. Copyright 1997, IEEE.

The output spectra at the receiver end under different system status are summarized and illustrated in Figure 6(b). Consider a fiber break in segment L_i between the $EDFA_{i-1}$ and the FBG_i, both data channels and monitoring wavelengths at λ_1 to λ_{i-1} are absent from the final spectrum since there is no signal being fed into $EDFA_i$ [Fig. 6(b), case(ii)]. As there is no ASE influence from $EDFA_{i-1}$, which is notched at λ_i, the FBG_i can reflect a stronger ASE at λ_i and thus the enhanced emission at λ_i will be pronounced. For the case of partial failure in $EDFA_{i-1}$, except the last EDFA in the system ($EDFA_N$), due to severe degradation in the pump laser diode and assuming no fiber break, there will be a reduction in the whole ASE spectrum as input to $EDFA_i$. The final spectrum is the same to that in case of fiber break in segment L_i, that is, a power enhancement at λ_i, except that the data channels are still present in this case [Fig. 6(b), case (iii)]. For a partial failure in the $EDFA_N$, there will be a significant power reduction in both data channels and monitoring wavelengths [Fig. 6(b), case (iv)].

Experiments based on the above scheme were carried out for a three EDFAs with an in-between amplifier spacing of 50 km [13]. Results generated agreed generally well with the proposed scheme. Currently, we are investigating the situation where many surveillance stages are cascaded to simulate the long haul transmission system using a fiber loop configuration.

3.2 Optical Branching Unit

The above discussed monitoring scheme can be extended to long haul transmission links where optical amplification and other functions are provided by individual branching units (BU) [14]. Our proposed BU [15] is equipped with add-drop capability and the health status of the EDFA can be continuously monitored.

Figure 7 shows the architecture of the proposed integrated WDM BU consisting of two sets of in-line Erbium-doped fibers (EDF) and two identical FBG with center wavelength at λ_i, *i* being the added and dropped data wavelength channel at BU_i. For optical amplification, EDF_1 is forward-pumped by PLD_1 while EDF_2 is backward-pumped by PLD_2. Note that our proposed configuration has two identical FBGs, which can help to reduce the in-band crosstalk at λ_i, a key issue of WDM system of similar add-drop design [16].

For fault detection, we only require an additional optical circulator inserted prior to FBG_2, and connected to the fault detection circuit as shown. The monitoring analysis is similar to those described in Fig. 6(b). Any failure in either pump laser diode can be identified in real-time.

3.3 Branched Optical Network

Figure 8 shows the surveillance scheme [17,18] for an M-ary passive branched optical networks (PBON) consisting of multiple 1xN stages. The FBG (centered wavelength outside EDFA's flat gain region) placed on each branch is used to slice and reflect the amplifier's ASE power at a designated wavelength other than the data signal wavelengths to form a monitoring channel for that branch. Thus, any great power drop in the reflected monitoring channel indicates the corresponding fiber link is failed.

We have demonstrated such concept with a 1x4 PBON using FBGs with center wavelengths at λ_1=1557.5 nm and λ_2=1559.9 nm. The 3-dB bandwidth and the reflectivity of each FBG are 0.9 nm and 90% respectively. Bit error rate measurements using 1-Gb/s (2^{10}-1 PRBS) NRZ data channel at 1555 nm with transmitted power 6 dBm shows no degradation in performance. To simulate a fiber break, the fiber is disconnected shortly prior to the FBG (separated by 6.6 km from the branching point) and a drop of a comfortable 9 dB in reflected monitoring power at the headend is observed, thus reported link failure.

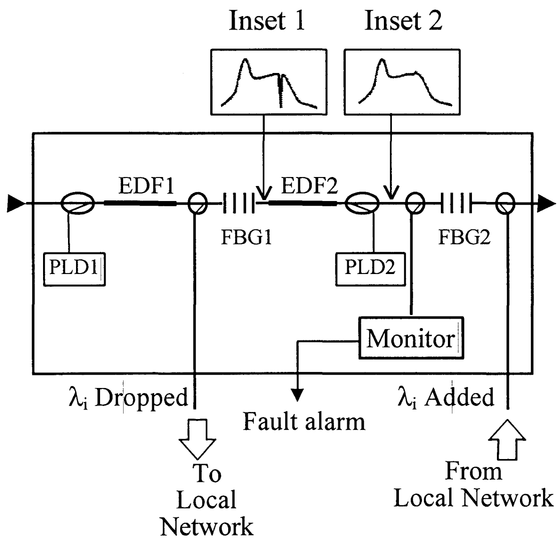

Fig. 7. Schematic of our proposed branching unit wit add-drop and monitoring capabilities. Reproduced with permission from Ref.15. Copyright 1998, IEE

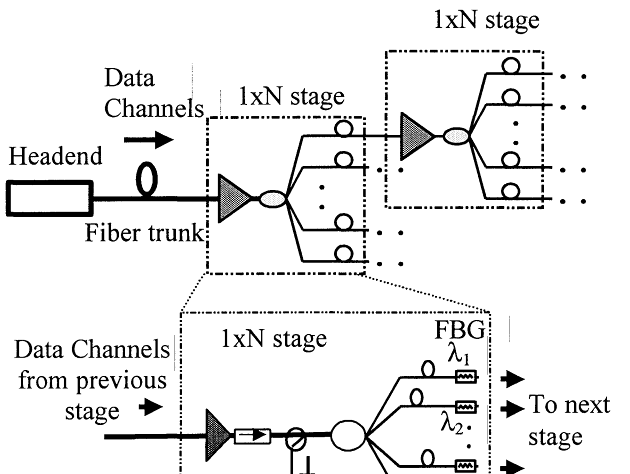

Fig. 8 Fault surveillance scheme for an M-ary tree-branched PBON. A 1xN stage PBON is shown in the inset. Reproduced with permission from Ref.17. Copyright 1997, IEEE.

4. A Proposed Supervisory Scheme for Wavelength Routing Network

Figure 9 illustrates our proposed hierarchical supervisory layers for a 5-node wavelength routing network. Wavelength routing network is chosen because of its significance and complexity, and variations of the same scheme can be adapted to other optical communication systems. The basic operational principle relies on continuously real-time monitoring of individual optical components and subsystems. Any fault developed can be identified immediately and the monitoring information will be sent for corrective actions. We propose to embed the surveillance information in the network signaling protocol, such as Common Channel Signaling No. 7 (CCS no. 7), with modifications in its user-defined fields. Thus the information can be transmitted in a separate and robust network.

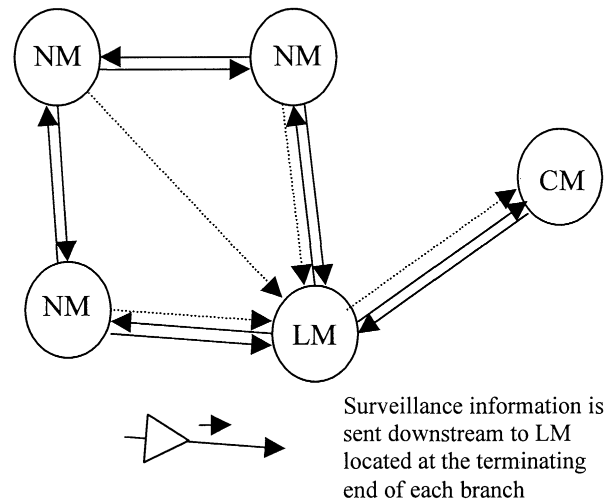

Figure 9. Hierarchical layers of the proposed supervisory scheme over a 5-node wavelength routing network. Solid lines are the fiber connections while dotted lines are the signaling and surveillance connections.

The four-layer hierarchical surveillance management includes the monitoring device (MD) layer at the bottom, node manager (NM) layer, local manager (LM) layer, and a single chairman (CM) layer at the top. The NM, LM, and CM are coincided with the wavelength routing nodes where wavelength channels will be added, dropped, or routed to other nodes through the OXC.

The MD layer provides the necessary monitoring information describing the types, locations, and timing of failure of the devices. Each of the network components, including OA, OXC, optical fiber segments, etc. is closely monitored, and the health status can either periodically be sent or polled by the NM located downstream from the components as shown. The NM will collect the surveillance information from all components on its incoming fiber links and submit to an assigned LM overlooking a number of routing nodes in a localized geographical area. The fault information collected by various LMs will finally be reported to a CM. With the health status and traffic loading of the entire network available, the CM issues proper actions, such as lightpath reconfiguration, in certain network routing nodes.

5. Summary

In summary, we have reviewed our previously proposed fault surveillance schemes that based on FBGs of different center wavelengths and the unused ASE spectrum of the EDFA as the sources. These schemes offer non-intrusive real-time surveillance functions continuously.

Surveillance scheme for an all-optical wavelength network that bases on surveillance of individual components is also discussed. We also propose the surveillance information can be carried in a modified network signaling protocol.

We would like to acknowledge the technical assistance from Eddie T.P. Kong, Ronald C.C. Hui, and Brian Sun. We are also thankful for the fiber Bragg gratings from JDS-FITEL, Inc.. The work is supported in part by UPGC-CUHK4140/97E.

References

1. S.B. Alexander, R.S. Bondurant, D. Byrne, V. W. S. Chan, S.G. Finn, R. Gallager, B.S. Glance, H.A. Haus, P.A. Humblet, R. Jain, I.P. Kaminow, M.J. Karol, R.S. Kennedy, A. Kirby, Han Q. Le, A.A.M. Saleh, B.A. Schofield, J.H. Shapiro, N.K. Shankaranarayanan, R.E. Thomas, R.C. Williamson, and R.W. Wilson, " A Scalable Multiwavelength Multihop Optical Network: A proposal for research on all-optical networks," IEEE/OSA J. Lightwave Tech. 11, 736-754 (1993).
2. G.R. Hill, P.J. Chidgey, F. Kaufhold, T. Lynch, O. Sahlen, M. Gustavsson, M. Janson, B. Lagerstron, G. Grasso, F. Meli, S. Johansson, J. Ingers, L. Fernandez, S. Rotolo, A. Antonielli, S. Tebaldini, E. Vezzoni, R. Caddedu, N. Caponio, F. Testa, A. Scavennec, M.J. O'Mahoney, J. Zhou, A. Yu, W. Sohler, U. Rust, and H. Herrmann, "A transport network layer based on optical network elements," IEEE/OSA J. Lightwave Tech. 11, 667-679 (1993).
3. S. Okamoto, A. Watanabe and K. Sato, "Optical path cross-connect node architectures for photonic transport network," IEEE/OSA J. Lightwave Tech. 14, 1410-1422 (1996).
4. J. L. Zyskind, Y. Sun, A. K. Srivastava, J. W. Sulhoff, A. J. Lucero, C. Wolf and R. W. Tkach, "Fast power transients in optically amplified multiwavelength optical networks," Technical Digest, OFC'96, Paper PD31-2, San Diego, CA, USA, (1996).
5. H. Takahashi, Y. Hibino, Y. Ohmori, and M. Kawachi, "Polarization independent arrayed-waveguide wavelength demultiplexer with birefringence compensating film," IEEE Photon. Tech. Lett. 5, 707-709 (1993).
6. C. S. Li, F. Tong, C. J. Georgio, and M. Chen, "Gain equalization in metropolitan and wide area optical networks using optical amplifiers," in Proceeding of IEEE INFOCOM (IEEE, 1994) 130-137.
7. C. K. Chan, F. Tong, and L. K. Chen, "Wavelength matching scheme for wavelength grating routers in all-optical transport networks," IEE Electron. Lett. 34, 490-491 (1998).
8. C. K. Chan, E. Kong, F. Tong, and L. K. Chen, "A novel path supervisory scheme for optical cross-connects in all-optical transport networks," IEEE Photon. Tech. Lett., 10, (1998).
9. F. Tong, K. P. Ho, T. Schrans, W. E. Hall, G. Grand, and P. Mottier, "A wavelength matching scheme for multiwavelength optical links and networks using grating demultiplexers," IEEE Photon. Tech. Lett., 7 680-690 (1995).
10. J. J. Pan, P. Ma, and Y. Shi, "Ultra-stable temperature compensated package of steep skirt grating for dense WDM," in Proceedings of NFOEC'97 (San Deigo, CA 1997).
11. Y. Inoue, A. Kaneko, F. Hanawa, H. Takahashi, K. Hattori, and S. Sumida, "Athermal silica-based arrayed waveguide grating (AWG) multiplexer," in Proceedings of IOOC-ECOC'97 (Edinburgh, UK, 1997), paper PD-TH3B-1.
12. Y. Hamazumi, and M. Koga, "Transmission capacity of optical path overhead transfer scheme using pilot tone for optical path network," IEEE/OSA J. Lightwave Tech. 15 2197-2205 (1997).
13. C. K. Chan, L. K. Chen, F. Tong, and D. Lam "A Novel in-service surveillance scheme for optically amplified transmission systems" IEEE Photon. Tech. Lett. 9, 1520-1522 (1997).
14. B. Pedersen, V.J. Mazurczyk, G.T. Harvey, G. Wolter, F.C. Bekampis and C.D. Anderson, "WDM branching unit for the new generation of undersea network system," in Proceedings of IOOC-ECOC97, (Edinburgh, UK, 1997), paper WE2A-7.
15. C. K. Chan, F. Tong, L. K. Chen and D. Lam, "A practical fault-monitored WDM branching unit for long-haul optical transmission systems" to appear in IEE Electron. Lett. (1998).
16. C. S. Li and F. Tong, Crosstalk and interference penalty in all-optical networks using static wavelength routers," IEEE/OSA J. Lightwave Tech., 14 1120-1126 (1996).
17. C. K. Chan, F. Tong, L. K. Chen, J. Song and D. Lam, "A practical passive surveillance scheme for optically-amplified passive branched optical networks," IEEE Photon. Tech. Lett., 9, 526-528 (1997).
18. C. K. Chan, F. Tong, L. K. Chen, and D. Lam, "In-service passive surveillance system for optically-amplified branched networks," IEE Elect Lett., 33, 795-797 (1997).